BIOCHEMICAL AND BIOPHYSICAL RESEARCH COMMUNICATIONS **251,** 61–66 (1998)
ARTICLE NO. RC989380

Conformational Change in an Anti-integrin Antibody: Structure of OPG2 Fab Bound to a β3 Peptide

Ramadurgam Kodandapani,[1] Leela Veerapandian,[2] Chao-Zhou Ni, Chu-Kuan Chiou, Randy M. Whittal,[3] Thomas J. Kunicki,* and Kathryn R. Ely[4]

*Cancer Research Center, The Burnham Institute, La Jolla, California 92037; and *Department of Vascular Biology and Department of Molecular and Experimental Medicine, Scripps Research Institute, La Jolla, California 92037*

Received August 3, 1998

Antibodies are important tools to explore receptor–ligand interactions. The anti-integrin antibody OPG2 binds in an RGD-related manner to the $\alpha_{IIb}\beta_3$ integrin as a molecular mimic of fibrinogen. The Fab fragment from OPG2 was cocrystallized with a peptide from the β_3 subunit of the integrin representing a site that binds RGD. The crystal structure of the complex was determined at 2.2-Å resolution and compared with the unbound Fab. On binding the integrin peptide there were conformational changes in CDR3 of the heavy chain. Also, a significant shift across the intermolecular interface between the C_H1-C_L domains was observed so that the angle of rotation relating the two domains was reduced by 15°. This unusual conformational adjustment represents the first example of ligand-induced conformational changes in the carboxyl domains of a Fab fragment.

Integrins are cell-surface receptors that mediate cell adhesion and cell-interactions (1, 2). These transmembrane glycoproteins are composed of α and β subunits that form non-covalent heterodimers; the formation of the ligand-binding site requires the contribution of sequences from both subunits. These receptors modulate a number of diverse cell-adhesion phenomena, often through recognition of the sequence arginine-glycine-aspartic acid (RGD). This recognition site was first identified in fibronectin (3, 4) but is also present in other matrix or adhesion proteins such as vitronectin or fibrinogen. Several integrins recognize the RGD sequence. Specific recognition of the RGD ligands by individual receptors is influenced by the conformation of the RGD tripeptide as well as amino acids in flanking sequences (5, 6). Cell adhesion ligands and integrins influence disease-related processes such as tumor cell invasion and metastasis or thrombosis and therefore synthetic peptides or mimetic compounds are potential agents for treatment of these disorders.

Antibodies are important tools to explore receptor-ligand interactions. When the antibodies are directed to the ligand-binding site of the receptor, the complementarity-determining regions (CDR) of the antibody may be conformationally similar to the receptor ligand. We previously determined the high resolution crystal structure of the antigen-binding fragment (Fab) from the OPG2 antibody (7) which is an anti-integrin antibody. This antibody (8) as well as two homologous antibodies; PAC-1 (9) and LJ-CP3 (10) are anti-receptor antibodies that bind specifically to the $\alpha_{IIb}\beta_3$ integrin. Each of these antibodies bears the sequence arginine-tyrosine-aspartic acid (RYD) in the CDR3 (H3) of the heavy chain. These antibodies are "molecular mimics" of fibrinogen since they inhibit binding of fibrinogen to the $\alpha_{IIb}\beta_3$ integrin on platelets. When the RYD sequences in the CDR3 loop was replaced by an RGD sequence, the OPG2 antibody retained specificity for the $\alpha_{IIb}\beta_3$ integrin (11); i.e., it bound selectively to $\alpha_{IIb}\beta_3$ and not to $\alpha_v\beta_3$. Moreover, it has been demonstrated for RGD-containing analogs of OPG2 and PAC-1 (AP7 and PAC-1.1) that sequences adjacent to the RGD sequence influence binding to resting or activated conformations of the platelet integrin (12).

We know from the crystal structure of OPG2 (7) that these Fabs are structural as well as functional mimics of natural RGD ligands. When compared to the structure of the fibronectin cell adhesion module (13) that contains the RGD tripeptide, we observed that there is

[1] Present address: Structural Biology Facility, Massachusetts General Hospital, Boston, MA.

[2] Present address: Department of Chemistry, University of California, San Diego, CA.

[3] Present address: Department of Pharmaceutical Chemistry, University of California, San Francisco, CA.

[4] To whom correspondence should be addressed at The Burnham Institute, 10901 North Torrey Pines Road, La Jolla, CA 92037. Fax: (619) 646-3196. E-mail: ely@burnham-inst.org.

Abbreviations used: RGD, arginine-glycine-aspartic acid; RYD, arginine-tyrosine-aspartic acid; CDR, complementarity-determining regions; Fab, antigen-binding fragment; NMR, nuclear magnetic resonance.

0006-291X/98 $25.00

a common molecular scaffold shared between the fibronectin module and the V_H domain of the OPG2 antibody (14). This unexpected structural homology means that the RGD sequences are located in structurally equivalent loops in the two proteins. The shared scaffold is used to present the tripeptide for receptor recognition.

In OPG2, a striking feature of the structure was the CDR3 (H3) loop which protrudes from the surface of the molecule (7). The RYD sequence was well ordered and located at the tip of this loop, at a distance of ~12 Å from the location of the combining site in other antibodies. Inspection of the atomic model revealed no prominent antigen-combining cavity suggesting that the antibody binds to the integrin as a ligand with a protruding loop that can interact with the receptor binding site. The RYD peptide is found in a "β-type" turn. The most interesting feature of this turn is the fact that the RYD sequence assumes two alternate conformations with equal occupancy. The conformational presentation of the RGD sequence is important for binding by specific integrins. The alternate conformations clearly defined in OPG2 may represent two conformations recognized by distinct receptors. On the other hand, the two conformations may correspond to alternate positions that the side chains assume in the free state versus when bound to integrin. To evaluate this hypothesis, we made a complex of the OPG2 Fab with a synthetic peptide from the β_3 subunit, focusing on the sequence around residue 119. This region was selected because a mutant receptor from a thrombasthenic patient has an interchange of D → Y at this position (15) and the mutant receptor fails to bind fibrinogen, RGD ligands and OPG2.

In this study, the Fab fragment from OPG2 was cocrystallized with the peptide from the β_3 subunit and the structure was solved at high resolution. Significant conformational changes were observed when the structures of the liganded and unliganded Fab were compared. On binding to the integrin peptide, there were conformational movements in the H3 loop of V_H. Also, binding to the integrin peptide caused a significant shift in the C_L-C_H1 modules of the Fab. The two domains shifted across the intermolecular interface so that the angle of rotation relating the two domains was reduced by nearly 15°. This conformational adjustment is highly unusual for antigen–antibody interactions and represents the first example where ligand-induced conformational changes are seen in the carboxyl domains of an Fab fragment.

MATERIALS AND METHODS

Crystallization. Two synthetic peptides were tested for cocrystallization with the OPG2 Fab. The peptides corresponding to residues 115-131 or a shorter peptide encompassing residues 119–131 from the β_3 subunit were synthesized using F-moc chemistry employing a Milligen Model 0.05 Pepsynthesizer (Milligen/Bioresearch). Peptides were purified to at least 95% homogeneity using a C18 reverse-phase HPLC column (Beckman Instruments, Inc.). The sequence of the longer peptide was: Tyr-Tyr-Leu-Met-Asp-Leu-Ser-Tyr-Ser-Met-Lys-Asp-Asp-Leu-Trp-Ser-Ile. OPG2 Fab was cleaved from the intact antibody with papain and purified as described previously (16). The peptides were mixed at 1:1 molar ratios with the Fab in 0.1 M sodium acetate, pH 5.5. The mixtures were tested for crystallization using conditions that produced large crystals of the native OPG2 Fab alone (imidazole-malate pH 5.8, PEG 1000, sodium chloride; (16)). In other trials, a sparse matrix sampling (17) was used to screen pH, buffers, and precipitants using the Crystalscreen I kit (Hampton, Inc.).

Crystallization trials were set up in hanging drops using the vapor diffusion method. Prismatic crystals formed at 22°C from solutions containing PEG 8000 in 0.1 M cacodylate, pH 6.5. Large crystals were obtained in one month under the following conditions: 2 μL protein/peptide solution at a concentration of 21 mg/ml was mixed with 2 μL of the reservoir solution (16% PEG 8000, 0.1 M cacodylate, pH 6.5, 0.2 M calcium acetate).

Mass spectrometry. To confirm the presence of peptide in the crystals, large crystals were washed extensively with the reservoir solution free of protein mother liquor and dissolved in trifluoroacetic acid/acetonitrile for mass analysis. Measurements were made using a Kratos Kompact MALDI 1-TOF mass spectrometer which has picomole sensitivity and a wide mass range capable of accurate mass calculations on samples such as the dissolved crystals which contain two components of vastly different mass (i.e., ~2,150 and 47,970 daltons respectively for the peptide and the Fab). To ensure accuracy, samples were measured in three independent runs with overlapping calibrations.

Data collection. X-ray diffraction data were collected from one crystal to 2.2-Å resolution using a Rigaku RU-200 rotating anode X-ray generator and two San Diego Multiwire Systems area detectors.

Structure solution. For phase calculation and structure solution, the molecular replacement method (18) was used. The starting probe model was the OPG2 Fab [Brookhaven Protein Data Bank (19) accession number 1OPG. Rotation searches were performed with the intact probe model and also with the V_L-V_H and C_L-C_H1 pairs. For the intact probe searches, the "elbow bend" angle was varied in X-PLOR (20). The rotation function search was followed by Patterson correlation refinement in X-PLOR. Translation function searches were done in X-PLOR for the orientations identified from the rotation function with a search grid of 1 Å. From these searches, a full model of the Fab was assembled and adjusted with rigid body refinement, positional refinement and simulated annealing in X-PLOR (21). Residues 101-110 in the heavy chain, corresponding to the third CDR (H3) were deleted in the model. Refinement with PROLSQ in GPRLSA (22, 23) was alternated with model building using FRODO (24) and O (25). Solvent atoms (312 atoms) were added to the model except in the region of the binding cavity and refinement continued 8.0 to 2.0 Å data. To identify the position of the peptide, $2F_o$-F_c difference maps and OMITMAPS (26) were implemented. Finally, the residues in the H3 loop were fitted to the model where clearly defined density was observed. The final coordinates have been submitted to the Brookhaven Protein Data Bank (19) under accession number 1bm3.

RESULTS AND DISCUSSION

Crystallization of the complex. For cocrystallization of the integrin peptide with the anti-integrin Fab, we selected a sequence from the β_3 subunit that had been previously shown to be critical for RGD ligand recognition by integrins that contain the β_3 subunit ($\alpha_{IIb}\beta_3$ or $\alpha_v\beta_3$). Experiments where RGD-containing peptides were crosslinked to the $\alpha_{IIb}\beta_3$ integrin localized the

region between residues 109–171 of the β_3 polypeptide in proximity to the ligand binding site (27). Within this region, a mutation at residue 119, substituting a tyrosine for aspartic acid caused complete loss of ligand binding (15). Because the OPG2 antibody binds to the $\alpha_{IIb}\beta_3$ integrin in an RGD-dependent manner, this sequence was chosen to begin the peptide binding studies. The goal was to crystallize a fragment of the integrin ligand-binding site in complex with the OPG2 ligand. Since the H3 CDR that bears the RGD site was ordered and well-defined in the crystal lattice, it was hoped that the crystal structure of the complex could provide data on the molecular contacts between the RGD sequence and the β_3 subunit.

Two synthetic peptides were synthesized to correspond to this region of the beta chain. One sequence consisted of residues 119 to 131 with the mutation site located at the amino-terminus of the peptide, while the second peptide was four residues longer beginning at residue 115 and extending to residue 131. When the short peptide was tested for complex cocrystallization using conditions that produced large crystals of the Fab alone [0.02 M imidazole-malate, pH 5.6, 0.16 M NaCl, PEG 1000; (16)], crystals with the morphology of native crystals appeared, suggesting that a complex had not been formed. In contrast, complexes formed with the larger peptide failed to crystallize under "native" conditions, but large crystals were obtained with quite different crystallization conditions: 0.1M cacodylate, pH 6.5, 0.2 M calcium acetate, and PEG 8000. Under these conditions, unliganded Fab failed to crystallize. Once large crystals were produced, they were washed extensively to remove all mother liquor and dissolved. The presence of both Fab and peptide in the crystals was confirmed by mass analysis using MALDI mass spectrometry (results not shown).

Large crystals formed in space group A2 with a = 74.11, b = 90.05, and c = 79.11 Å and β =115.3°. Diffraction data were collected from a single crystal to 2.0-Å resolution.

Structure solution. The structure of the OPG2 Fab in complex with the β3 peptide was determined at 2.0-Å resolution by molecular replacement methods. The final R factor for 8.0–2.0 Å data was 0.15 after refinement of 3377 protein atoms and 312 solvent atoms. The final refinement statistics are presented in Table I. The structure of the Fab was well-defined except for residues 102–107 in CDR3 (H3) of the heavy chain. Disappointingly, there was no clearly defined density for the peptide. (To absolutely verify that the peptide was bound to the protein in the crystal, final mass spectrometric analysis was performed on the actual crystal used for data collection, and the presence of both Fab and peptide was confirmed; data not shown). There is a head-to-tail packing of the Fabs in the crystal lattice and there is ample room for the peptide to be accommodated so the lack of defined density is probably not due to steric limitations and crystal lattice interactions.

TABLE I

Refinement Statistics

	Final	Target
Resolution range (Å)	8.0–2.0	
Average B (Å^2)	27.7	
Crystallographic R-factor (%)	15.2	
Number of reflections used	20334 $> 3\sigma$(F)	
Number of atoms	3377	
Number of waters	312	
RMS deviation from ideal distances (Å)		
Bond distances	0.017	0.020
Angle distances	0.062	0.045
Planar 1–4 distances	0.041	0.035
RMS deviation from ideal planarity (Å)	0.015	0.020

In the unliganded OPG2 Fab (7), the entire molecule was clearly determined including the H3 loop which was a striking feature of the Fab. This loop, consisting of residues 101–110, protruded from the surface of the molecule. The RYD sequence was located at the tip of this loop about 12 Å from the location of the combining site in other antibodies. During the examination of the structure of the unliganded OPG2 molecule, we noticed that the Fab had no prominent binding cavity and proposed that the antibody binds to the integrin as a ligand with a protruding loop that can interact with the receptor binding site. Comparison of this H3 loop in the liganded and unliganded Fab suggests that this loop is flexible and that a conformational rearrangement of the RYD(RGD) loop may occur on binding integrin. Since there is no actual combining cavity in the antibody, there is no crevice for the peptide to bind. If principal contacts between the integrin sequence and the antibody are mediated by the H3 loop, then it is possible that flexibility in this loop could permit a range of conformations and consequently a range of locations for the bound peptide. In this case, there would be no clearly defined density for the peptide or the flexible regions of the H3 loop. There are precedents for conformational adjustments of more that 5 Å in the H3 loop upon ligand binding of two anti-viral antibodies (28, 29). In both of these studies there was a large rearrangement of the CDR3 of the heavy chain to accommodate the ligand.

Conformational changes in the integrin-bound form of the OPG2 Fab. While there were major conformational adjustments in the H3 loop of OPG2 when peptide bound, there were less dramatic changes in the other five CDR loops in the Fab. When the five clearly defined CDRs were superimposed, the overall rms deviation between corresponding α-carbons was 0.64 Å. As shown in Fig. 1, the major differences between the

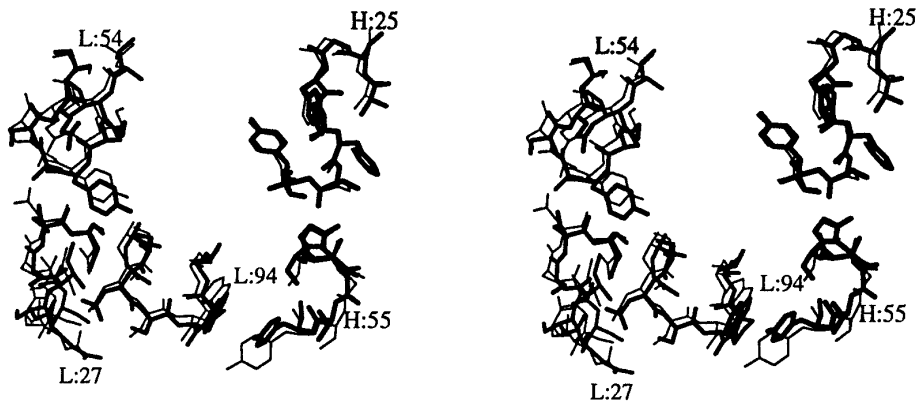

FIG. 1. Comparison of CDR loops in the antigen-combining site in the bound and unbound form of OPG2. In this stereoplot, residues for five CDR loops that were ordered and visible in the electron density map are superimposed: thick lines represent atoms from the peptide-bound OPG2 and thin lines correspond to atoms from the unliganded OPG2. Selected residues are labeled for identification of the loops. Residues shown in the figure for the light chain are CDR1, residues L25 to L32; CDR2, residues L47 to L54, CDR3, residues L90 to L96. For the heavy chain residues for two loops are shown: CDR1, residues H24 to H32 and CDR2, residues H51 to H57. Note that the positions of the backbone atoms in these five CDRs are closely similar. This observation and the fact that CDR3 from the heavy chain undergoes significant conformational changes on binding peptide suggests that the principal contacts for the peptide are made by CDR3.

loops in the bound and free forms were in the relative positions of side chains. In particular, aromatic side chains in H2, L2, and L3 shifted when ligand was bound. The location of the hydroxyl groups of tyrosines H57 and L50 differed by 6.4 and 1.08 Å, respectively, and the position of tryptophan L94 (measured at atom CH2) shifted by 2.6 Å.

The pseudo-twofold rotation axes relating variable and constant domain pairs of the unliganded and liganded OPG2 Fabs, as well as the "elbow bend" angle between the V and C domain pairs are listed in Table II. When the two Fabs are superimposed the rms deviation between corresponding α-carbons is 1.68 Å (for 432 α-carbons excluding residues 101–109 in the H3 loop). When just the Fv fragments (i.e., V_L-V_H domain pairs) were superimposed, the positions of 227 α-carbons overlapped with an rmsd = 0.54 Å. In contrast, when the C_L-C_H 1 domain pairs were superimposed the average rmsd was 1.03 Å. The differences in the positions of corresponding atoms in the C domain pairs reflect the fact that the quaternary organization of the C domains is strikingly different in the two antibodies. As listed in Table II, the pseudotwofold rotation angles relating the C domains are quite different (13°). The rotation angle relating V domain pairs differs by ~8°. The overall folding patterns of the liganded and unliganded Fabs are compared in Fig. 2. When viewed in the orientation in the lower panel in this figure, it could be assumed that the "elbow angle" relating the V and C pairs changes when ligand is bound, however, as tabulated in Table II, the "elbow angles" differ by only 2° in the two Fabs. Since the rmsd for comparable α-carbons is greater in the overlapped C domain pairs than in the V domain pairs, and the difference in the rotation angle relating the light and heavy chain C domains is greater than the rotation angle relating V domains, the results suggest that OPG2 undergoes a conformational change on binding the integrin peptide and that this change is reflected principally in the quaternary orientation of the C domains.

TABLE II

Comparison of Rotation Axes and "Elbow Bend" Angles for the Bound and Unbound Form of OPG2 Fab

Axis or angle	OPG2 bound	OPG2 unbound
V_LV_H pseudotwofold	178°	169°
C_LC_H pseudotwofold	159°	172°
Elbow bend angle	152°	150°

Conformational changes on ligand binding frequently are observed in the H3 loop in the V domain of the heavy chain and also in the relative arrangement of the V_H-V_L domains (reviewed in Ref. 30). It is more unusual to observe conformational differences involving the C domains in comparisons of the bound and unbound forms of antibodies. In one study, upon binding of a small ligand, the C domain pair of the NC6.8 Fab was displaced by 19°, but this shift was also accompanied by a 31° change in the "elbow bend" angle (31). With OPG2, the conformational differences between liganded and unliganded forms are principally located in the C domains with a shift that affects the interdomain interactions between the domains without significant change in the "elbow bend". To our knowledge, this is the first indication of rearrangement of the quaternary packing of C domains in the liganded form of an antibody.

With regard to the conformational change in the H3

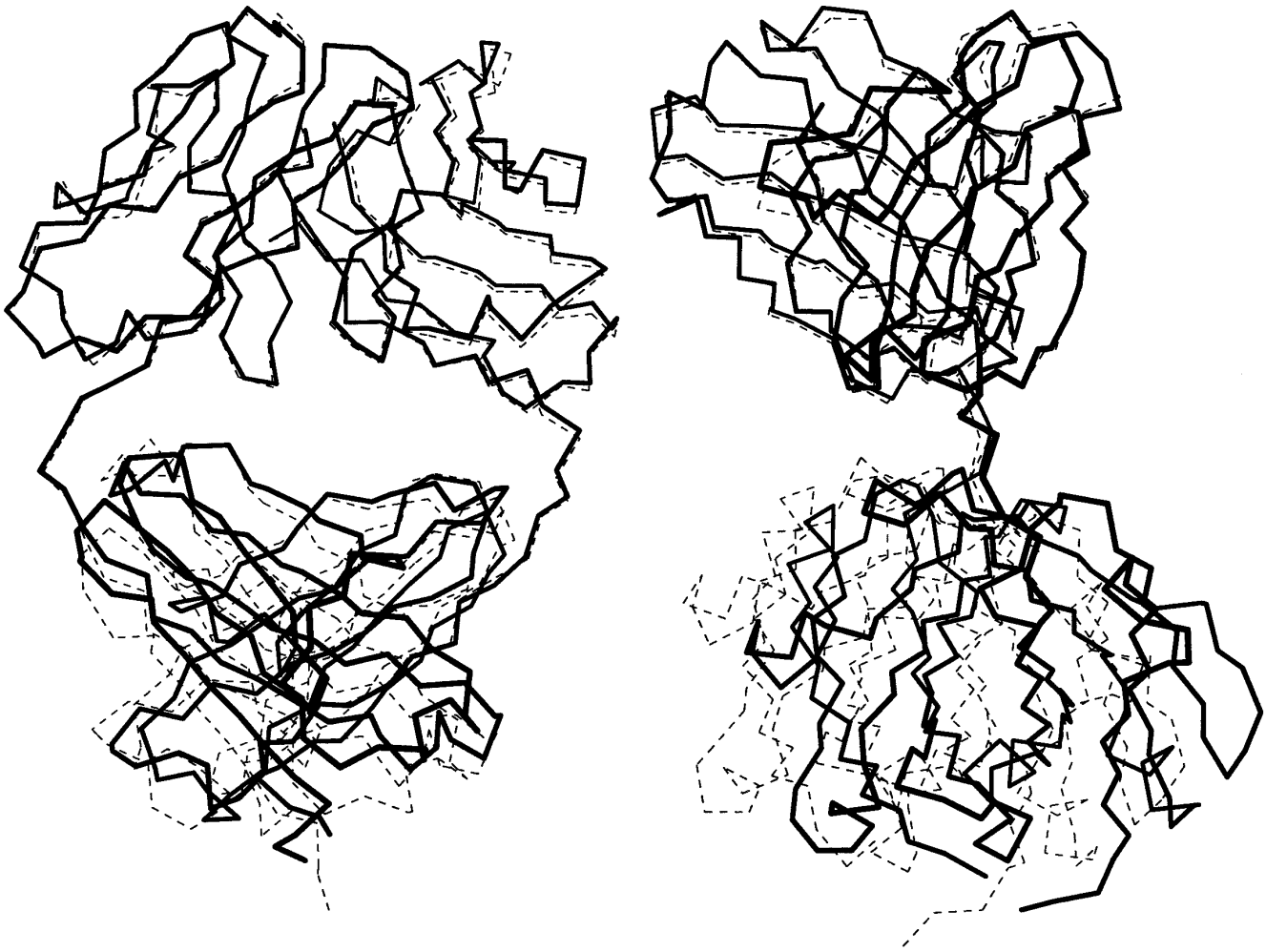

FIG. 2. Schematic representation to compare the polypeptide backbone of the bound and unbound form of OPG2 Fab. The images represents the α-carbon backbones for the two crystal forms with thick lines corresponding to OPG2 bound to peptide and thin lines corresponding to the unbound form. For this figure the α-carbons for the V_HV_L domain pairs (toward the top in each panel) were superimposed. The two views represent this superimposition as seen after a 90° rotation of the top view to generate the view in the right panel. In the latter view, the dramatic shift in the C_L-C_H1 pairs is evident.

CDR loop upon peptide binding, the fact that this loop becomes disordered in the Fab-peptide complex suggests that the peptide is bound directly to the H3 loop with few interactions with other CDR loops in the Fab. In one study of the Fab-peptide complex of a monoclonal antibody raised against HIV-1 protease, an intermolecular antiparallel β-sheet was formed between the peptide and the H3 loop and significant conformational changes occurred in this CDR with peptide binding (32). On the other hand, CDR H3 of the antitumor antibody BR96 did not undergo conformational changes on antigen-binding even though there were significant contacts made by this loop with the carbohydrate antigen (33).

Perhaps the flexibility induced in the H3 loop of OPG2 results from the fact that this antibody is a mimic of functional cell adhesion molecules such as fibronectin or disintegrins, with a common structural scaffold for presentation of the RGD sequence (14). In these molecules the RGD sequence is frequently located at the tip of a flexible loop. Recently the structures of the free and antibody-bound form of the RYD sequence from the *Leishmania* surface glycoprotein gp63 were determined by NMR (34). Interestingly, the backbone conformations of the free and bound RYD peptides were closely similar to the two conformations seen in OPG2 (7).

Within the class of immunoglobulins, the H3 loop of the OPG2 Fab belongs to a small subset of molecules where the loop extends well away from the combining site (35, 36). This feature may permit close penetration of the ligand mimic into the ligand binding site on the integrin. The unusual re-orientation of the C domains in OPG2 on peptide binding suggests that anti-receptor antibodies that mimic ligands and actually bind in the recognition pocket of the receptor may not exhibit the

conformational adjustments typically seen in antibodies that undergo an induced fit of antigen in the combining site.

ACKNOWLEDGMENTS

This work was supported in part by Grant CA28896 from the National Institutes of Health. The authors are grateful to Paula Kovack for preparing the manuscript for publication.

REFERENCES

1. Hynes, R. O. (1992) *Cell* **69,** 11–25.
2. Ruoslahti, E. (1991) *J. Clin. Invest.* **87,** 1–5.
3. Pierschbacher, M. D., and Ruoslahti, E. (1984) *Nature* **309,** 30–33.
4. Pierschbacher, M. D., and Ruoslahti, E. (1987) *J. Biol. Chem.* **262,** 17294–17298.
5. Ruoslahti, E., and Pierschbacher, M. D. (1987) *Science* **238,** 491–497.
6. Obara, M., Kang, M. S., and Yamada, K. M. (1988) *Cell* **53,** 649–657.
7. Kodandapani, R., Veerapandian, B., Kunicki, T., and Ely, K. R. (1995) *J. Biol. Chem.* **270,** 2268–2273.
8. Tomiyama, Y., Tsubakio, T., Piotrowicz, R. S., Kurata, Y., Loftus, J. C., and Kunicki, T. J. (1992) *Blood* **79,** 2303–2312.
9. Taub, R., and Greene, M. I. (1992) *Biochemistry* **31,** 7431–7435.
10. Niiya, K., Hodson, E., Bader, R., Byers-Ward, V., Koziol, J. A., Plow, E. F., and Ruggeri, Z. M. (1987) *Blood* **70,** 475–483.
11. Kunicki, T. J., Ely, K. R., Kunicki, T. C., Tomiyama, Y., and Annis, D. S. (1995) *J. Biol. Chem.* **270,** 16660–16665.
12. Kunicki, T. J., Annis, D. S., Deng, Y.-J., Loftus, J. C., and Shattil, S. J. (1996) *J. Biol. Chem.* **271,** 20315–20321.
13. Dickinson, C. D., Veerapandian, B., Ni, C.-Z., Dai, X.-P., Xuong, N.-H., Hamlin, R., Ruoslahti, E., and Ely, K. R. (1994) *J. Mol. Biol.* **236,** 1079–1092.
14. Ely, K. R., Kunicki, T. J., and Kodandapani, R. (1995) *Protein Eng.* **8,** 823–827.
15. Loftus, J. C., O'Toole, T. E., Plow, E. F., Glass, A., Frelinger, A. L., III, and Ginsberg, M. H. (1990) *Science* **249,** 915–918.
16. Celikel, R., Willimason, M. M., Ni, C.-Z., Kunicki, T. J., and Ely, K. R. (1993) *Acta Crystallogr.* **D49,** 421–422.
17. Jancarik, J., and Kim, S.-H. (1991) *J. Appl. Crystallogr.* **24,** 409–411.
18. Rossmann, M. G. (1972) The Molecular Replacement Method: International Science Review, New York, Vol. 13, Gordon and Breach, NY.
19. Bernstein, F. C., Koetzle, T. F., Williams, G. J., Meyer, E. E. J., Brice, M. D., Rodgers, J., Kennard , O., and Shimanouchi, T. (1977) *J. Mol. Biol.* **112,** 535–542.
20. Brünger, A. T. (1992) X-PLOR Manual, Yale University, New Haven, CT.
21. Brünger, A. T. (1988) *J. Mol. Biol.* **230,** 803–816.
22. Hendrickson, W. A. (1985) *Methods Enzymol.* **115,** 252–270.
23. Furey, and Swaminathan. (1990) *in* American Crystallographic Association Meeting Vol. 18, pp. 33, New Orleans, LA.
24. Plfugrath, J. W., Saper, M. A., and Quiocho, F. A. (1984) *in* Methods and Applications in Crystallographic Computing (Hall, S., and Ashiaka, T., Eds.), pp. 404–407, Clarendon Press, Oxford, NY.
25. Jones, T. A., Zou, J.-Y., Cowan, S. W., and Kjeldgaard, M. (1991) *Acta Crystallogr.* **47,** 110–119.
26. Bhat, T. N., and Cohen, G. H. (1984) *J. Appl. Crystallogr.* **17,** 244–248.
27. D'Souza, S. E., Ginsberg, M. H., Lam, S. C., and Plow, E. F. (1988) *J. Biol. Chem.* **263,** 3943–3951.
28. Smith, T. J., Chase, E. S., Schmidt, T. J., Olson, N. H., and Baker, T. S. (1996) *Nature* **383,** 350–354.
29. Rini, J. M., Schulze-Gahmen, U., and Wilson, I. A. (1992) *Science* **255,** 959–965.
30. Guddat, L. W., Shan, L., Fan, Z.-C., Andersen, K. N., Rosauer, R., Linthicum, D. S., and Edmundson, A. B. (1995) *FASEB J.* **9,** 101–106.
31. Wilson, I. A., and Stanfield, R. L. (1994) *Curr. Opin. Struct. Biol.* **4,** 857–867.
32. Lescar, J., Stouracova, R., Riottot, M. M., Chitarra, V., Brynda, J., Fabry, M., Horejsi, M., Sedlacek, J., and Bentley, G. A. (1997) *J. Mol. Biol.* **267,** 1207–1222.
33. Sheriff, S., Chang, C.-Y. Y., Jeffrey, P. D., and Bajorath, J. (1996) *J. Mol. Biol.* **259,** 938–946.
34. Petit, M.-C., Orlewski, P., Tsikaris, V., Sakarellos-Daitsiotis, M., Sakarellos, C., Tzinia, A., Konidou, G., Soteriadou, K. P., Marraud, M., and Cung, M. T. (1998) *Eur. J. Biochem.* **253,** 184–193.
35. Vix, O., Rees, B., Thierry, J.-C., and Altschuh, D. (1993) *Protein Struct. Funct. Genet.* **15,** 339–348.
36. He, X. M., Ruke, R. F., Casale, E., and Carter, D. C. (1992) *Proc. Natl. Acad. Sci. USA* **89,** 7154–7158.